Available online at www.sciencedirect.com
SCIENCE DIRECT
Thin Solid Films 514 (2006) 254–257
thin solid films
www.elsevier.com/locate/tsf

Effect of buffer layer on minority carrier lifetime and series resistance of bifacial heterojunction silicon solar cells analyzed by impedance spectroscopy

Germà Garcia-Belmonte [a,*], Jorge García-Cañadas [a], Ivan Mora-Seró [a], Juan Bisquert [a], Cristóbal Voz [b], Joaquim Puigdollers [b], Ramon Alcubilla [b]

[a] Departament de Ciències Experimentals, Universitat Jaume I, E-12071 Castelló, Spain
[b] Departament d'Enginyeria Electrònica, Universitat Politècnica de Catalunya, E-08034 Barcelona, Spain

Received 22 November 2005; received in revised form 7 February 2006; accepted 10 February 2006
Available online 6 March 2006

Abstract

By combining information on solar cell layer structure and electrical response analyzed by impedance spectroscopy, relevant knowledge is obtained about photogenerated carriers recombination and extraction. The inclusion of a-Si:H buffer layers on the response of bifacial heterojunction silicon solar cells prepared by hot-wire chemical vapor deposition is studied. Impedance analysis indicates that the effect of the buffer layer is twofold: (a) effective minority carrier lifetime is improved by one order of magnitude, confirmed by alternative quasi-steady-state photoconductance, and (b) whole series resistance is increased. Both effects seem to compensate each other so as to get similar efficiency and fill factor.

Keywords: Solar cell; Impedance spectroscopy; Buffer layer; Chemical vapor deposition; Carrier lifetime

1. Introduction

The static current–voltage characteristic of solar cells is routinely used to extract fundamental cell parameters and check device performance. It has been seldom recognized [1–4] that useful knowledge may be gathered by analyzing ac characteristics of solar cells in addition to dc curves. Impedance spectroscopy (IS) measurements taken over a broad frequency range (Hz–MHz) provide information on any system that is composed of a combination of interfacial and bulk processes, such as transport, recombination and interfacial states in solar cells [5]. The experimental method is straightforward but the interpretation of the results needs detailed models for assessing the mechanisms involved.

Simple ac equivalent circuits of solar cells should incorporate the capacitive effect corresponding to the excess minority carriers (C_d usually denoted the diffusion capacitance) in parallel with the depletion layer capacitance C_j (see Fig. 1a) [6]. Resistive effects arise from the minority carrier recombination R_r [7] and shunt resistances R_t. An additional series resistance is needed to model the contact effect R_s. In the forward bias direction the diffusion capacitance increases due to the minority carrier accumulation in the absorber layer and excess the junction capacitance, $C_d > C_j$ [8]. The ac equivalent circuit in this situation is represented in Fig. 1b, assuming also $R_t \gg R_r$. This simple equivalent circuit behaves like a parallel RC subcircuit in series with R_s. It is expected that impedance contributions from layers in which transport is determined by majority carriers are assimilated into R_s. However, intrinsic buffer layers can contribute with additional subcircuits despite their thickness in the nanometer scale (Fig. 1c), in which C_b and R_b account for the dielectric and resistive response of the buffer layer, respectively.

In this work we show that impedance spectroscopy provides detailed information on the factors determining the photovoltaic efficiency of different configurations of bifacial heterojunction

* Corresponding author. Tel.: +34 964 728023; fax: +34 964 728066.
E-mail address: garciag@uji.es (G. Garcia-Belmonte).

0040-6090/$ - see front matter © 2006 Elsevier B.V. All rights reserved.
doi:10.1016/j.tsf.2006.02.020

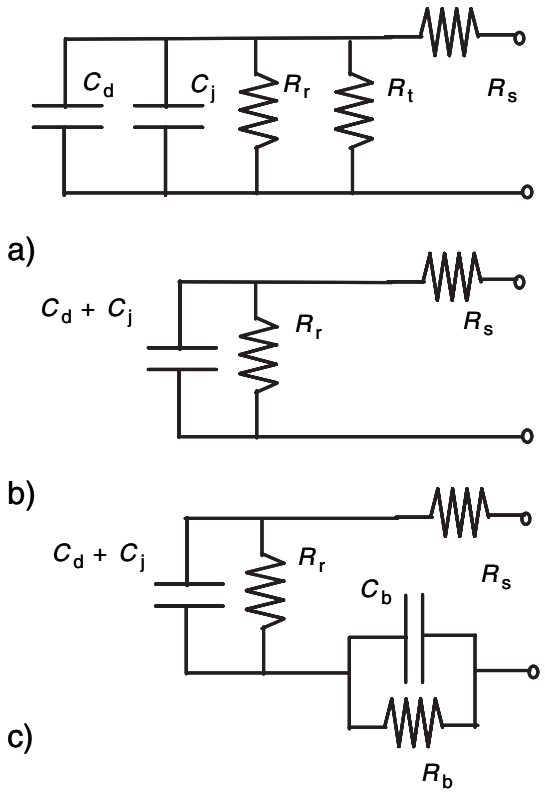

Fig. 1. (a) General solar cell ac equivalent circuit. (b) Simplification in case of $R_t \gg R_r$. (c) Additional contributions from intrinsic buffer layers.

thin film silicon solar cells. These devices are an excellent alternative for the fabrication of high efficiency silicon solar cells in an entirely low temperature fabrication process [9–12]. However, knowledge about transport and recombination mechanisms taking part in this device is still incomplete. Then, IS measurements can offer a new and valuable insight into the interface between crystalline and amorphous silicon.

2. Sample preparation and experimental conditions

The heterojunction silicon solar cells studied in this work are obtained on p-type polished float zone silicon wafers (100) of thickness 400 μm following a method described elsewhere [13]. The inner structure of the studied solar cells is summarized in Table 1, with all the films deposited by hot-wire chemical vapor deposition technique [14]. In both cases, the solar cells are defined with an area of 1.4 cm^2 by sputtering 90-nm thick indium tin oxide (ITO) layers onto the emitter and back contact. The front grid and back contact are obtained by evaporating silver in high vacuum. Then, the main structural difference between Cells A and B is the inclusion of hydrogenated amorphous silicon (a-Si:H) buffer layers in the second case. Therefore, IS measurements are performed in order to study the effect of including a 5-nm thick buffer layer. As we will next show the buffer layer improves the effective minority carrier lifetime τ_{eff} by more than one order of magnitude. However, this intrinsic buffer layer increases the whole series resistance with an additional term R_b (Fig. 1c). For the studied configurations, both effects seem to compensate each other so as to get similar cell parameters for efficiency and fill factor (FF).

Table 1
Heterostructures analyzed in this work

Cell name	Emitter		Back contact	
	n-doped	Intrinsic	Intrinsic	p-doped
A	μc-Si:H (50 nm)	–	–	μc-Si:H (50 nm)
B	a-Si:H (50 nm)	a-Si:H (5 nm)	a-Si:H (5 nm)	μc-Si:H (50 nm)

The impedance measurements were carried out using an Autolab PGSTAT-30 equipped with a frequency analyzer module in the frequency range between 1 MHz and 1 Hz. Ac oscillating amplitude was as low as 10 mV (rms) in order to maintain the linearity of the response. Impedance spectra were recorded either in the dark under varying bias voltage or in open circuit conditions under varying illumination from 0.05 sun up to 1.5 sun. This last measuring procedure yields a more homogeneous distribution of excess minority carriers because dc current is not allowed.

3. Results and discussion

As observed in Fig. 2 the incorporation of buffer layers increases the value of the open-circuit potential (V_{oc}) from 546 mV (Cell A) up to 577 mV (Cell B). As known, V_{oc} is related to the excess carrier density, what implies higher electron density in Cell B than in Cell A for 1 sun irradiance level. This is in fact an expected result because buffer layers inhibit to some extent the charge carrier recombination. On the other hand, the short-circuit current is slightly higher for Cell A (27.7 mA cm^{-2}) than for Cell B (24.2 mA cm^{-2}). However, this difference is probably due to a better quality of the ITO antireflecting coating in Cell A. In conclusion, both solar cells yield a conversion efficiency of around 9% with FF over 60%.

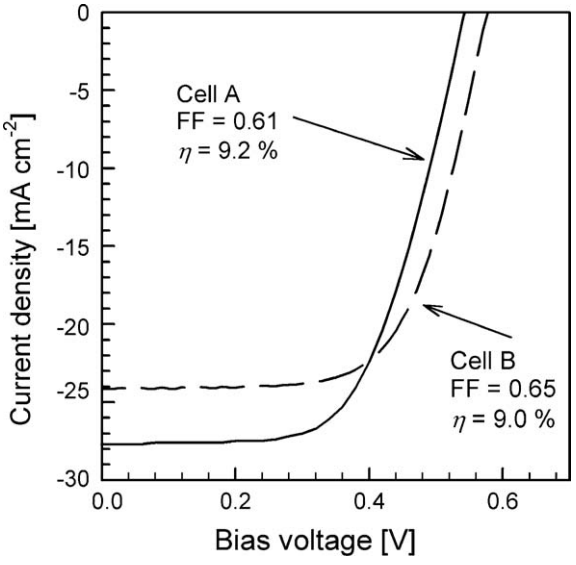

Fig. 2. Current–voltage characteristics of bifacial heterojunction solar cells measured under 1 sun-irradiance (1000 W m^{-2}) conditions. (solid line) Cell A and (dashed line) Cell B.

General capacitive response of both cells was firstly checked to verify that the diffusion capacitance is clearly distinguishable from the depletion capacitance in the forward bias direction. We measured the device capacitance at low frequencies (1 kHz) in dark conditions. By examining Fig. 3 one can readily observe that depletion-layer capacitance is visible at lower bias voltages. In this voltage region measured capacitance behaves as $C^{-2} \propto V_{bias}$, as expected for a depletion layer capacitance (inset of Fig. 3). Flatband potential of each junction can be calculated from the linear fits and result for Cell A equal to 0.76 eV, and 0.96 eV for Cell B. This is in agreement with the higher open-circuit potential value reported for Cell B. The increase in the flatband potential observed for Cell B may be related to the potential drop associated to the insulating layer. For potentials more positive than 0.4 V, diffusion capacitance dominates exhibiting the standard exponential dependence with bias potential. At potentials ~0.6 V, the diffusion capacitance seems to saturate. This effect is commonly attributed to the series resistance potential drop, which has a dramatic influence as device dc current increases in the forward direction.

Impedance spectra measured under 1 sun irradiance are shown in Fig. 4. Spectrum corresponding to Cell A (no buffer layers) can be understood in terms of the equivalent circuit of Fig. 1b. In this case a contact series resistance of 1.58 Ω cm^2 is observed. The low-frequency part is dominated by the *RC* subcircuit that draws a semicircle in a Z'–Z'' complex plot. The recombination resistance results in R_r=0.24 Ω cm^2. The response time of such subcircuit τ can be readily used to calculate the effective lifetime, $\tau_{eff}=R_rC_d=\tau-R_rC_j$, provided that the depletion layer capacitance is known from measurements shown in Fig. 3. The frequency corresponding to the maximum reached by the imaginary part of the complex impedance signals the response time inverse, as indicated in Fig. 4. Alternatively, τ can be also read from the peak of the Z'' vs. f plot. By contrast, the impedance spectrum is rather different for cell B where, instead of a simple semicircle, two well-defined arcs are present. This suggests the equivalent circuit of Fig. 1c as more suitable to interpret the response. The elements corresponding to the arc at high frequencies, R_b and C_b, appear potential-independent. It is observed that R_b decreases slightly with irradiance in the range of 10–13 Ω cm^2. The origin of the small arc at low-frequencies can be attributed to excess charge carrier accumulation and recombination, as discussed for Cell A. Recombination resistance results much higher (R_r ~2 Ω cm^2) compared to that measured for Cell A.

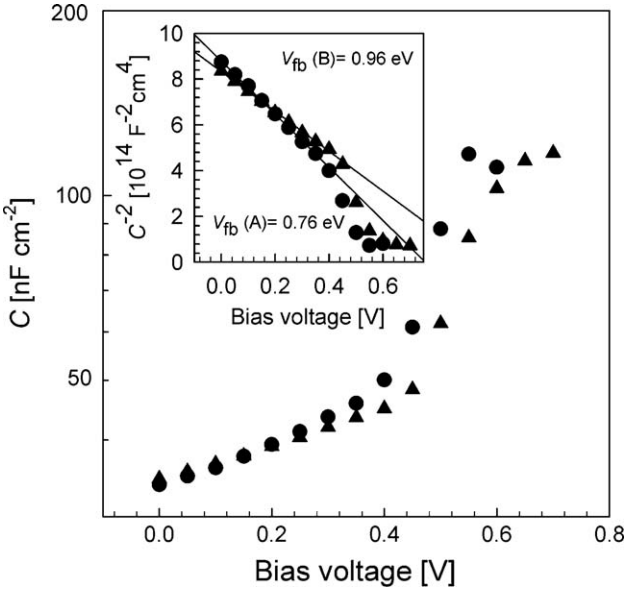

Fig. 3. Cell capacitance measured at 1 kHz as a function of the bias voltage in the dark. (●) Cell A and (▼) Cell B. In the inset: $1/C^2$ vs. V_{bias} analysis showing the flatband potential calculated from the linear fit intercept.

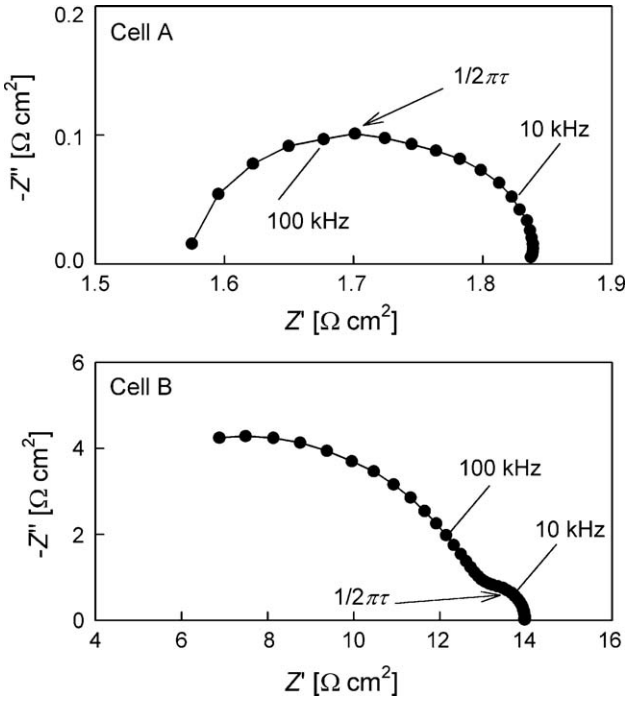

Fig. 4. Impedance spectra (Z'–Z'' complex plot) of bifacial heterojunction solar cells measured under 1 sun-irradiance (1000 W m^{-2}) and open-circuit conditions. Characteristic frequency $1/2\pi\tau$ is signaled with an arrow. Some other frequencies are also marked.

A simple method to compare effective lifetime values of both cells is therefore the determination of the response time, as indicated by an arrow in each spectra, under irradiation variation in open-circuit conditions. Results are presented in Fig. 5 for different illumination levels. As expected by effect of the buffer layer, Cell B exhibits longer τ_{eff} values in more than one order of magnitude. It should be stressed that these results are in good agreement with direct τ_{eff} measurements performed previously by the quasi-steady-state photoconductance (QSS-PC) technique [15], so as to confirm the validity of our approach.

As suggested previously, the additional arc appearing in Cell B impedance spectra at high frequencies must be related to the electrical response of the thinner buffer layer near the emitter. Other possibilities, like seeing the emitter layer itself as responsible for this additional subcircuit, can be safely discarded. Although emitter differs in structure between both cells, it is rather hard to expect a resistance contribution of about

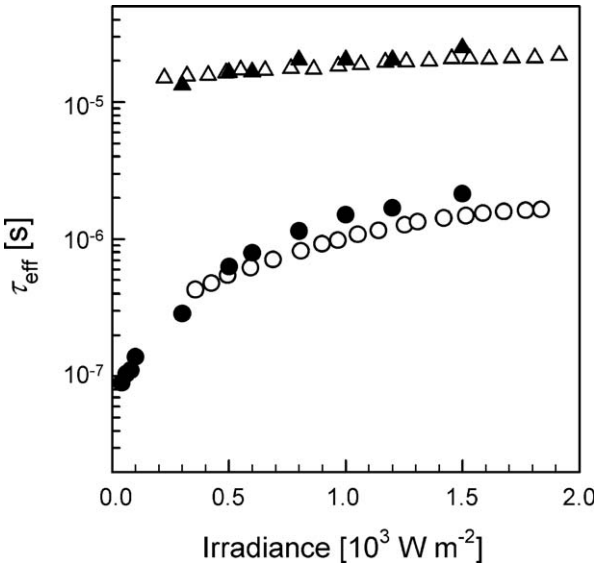

Fig. 5. Effective minority carrier lifetime calculated from impedance measurements (filled) compared with alternative QSS-PC results (empty) as a function of irradiance. (●) Cell A and (▼) Cell B.

12 Ω cm^2 from doped layers only 50-nm thick. Furthermore, we can assure that the additional arc is due from the response of the intrinsic buffer layer by determining the relative permittivity resulting from the measured capacitance value C_b=0.7 μF cm^{-2}, which is irradiance and voltage-independent. Relative permittivity gives $\varepsilon \approx 4$ in good agreement with the value usually reported for a-Si:H [8]. The conductivity of the intrinsic buffer layer can be thereby calculated and results $\sigma \approx 4.2 \times 10^{-8}$ Ω^{-1} cm^{-1}. It is known that intrinsic amorphous silicon has a conductivity value of the order of 10^{-9} Ω^{-1} cm^{-1} at room temperature in the dark [14]. Tacking into account that the buffer layer is only 5-nm thick and is placed between highly doped materials, it is expected a shift of the Fermi level. Moreover, impedance measurements were performed under illumination. The combination of these two effects suffices to explain the measured value for the intrinsic layer conductivity. A well-established order of magnitude for the amorphous silicon mobility is 1 cm^2 V^{-1} s^{-1} [16]. This allows calculating an estimation of the doping level of the intrinsic layer, which results reasonably in the order of 10^{11} cm^{-3}.

Since the additional, high-frequency arc yields the main contribution to the cell B resistance at high illuminations, the overall series resistance is then increased as a consequence of the buffer layer inclusion. Then, effective lifetime and series resistance increments produced by the buffer layer contribute in opposite ways to the solar cell performance. In fact, both effects seem to compensate each other in the studied solar cells resulting in similar cell parameters for conversion efficiency and FF.

4. Conclusions

Impedance spectroscopy measurements taken over a broad frequency range are able to provide useful information on minority carrier recombination and the effect of buffer layers on carrier extraction in heterojunction silicon solar cells. The analysis is based on simple *RC* subcircuits resulting from different cell layers and electronic mechanisms. IS measurements confirm that, as expected, the buffer layer reduces minority carrier recombination. However, buffer layers have the drawback of increasing the series resistance. Finally, τ_{eff} values can be deduced from impedance spectra in complete devices, evidencing excellent agreement with QSS-PC measurements in device precursors.

Acknowledgments

Financial support form *Ministerio de Ciencia y Tecnología* under project MAT2004-05168 and the *Comisión Interministerial de Ciencia y Tecnología* (CICYT) under programme ENE2004-07376-C03-01, both of the Spanish Government, is acknowledged. This work was developed in the framework of the *Centre de Referència en Materials Avançats per a l'Energia* (CeRMAE) of the *Generalitat de Catalunya*.

References

[1] R. Anil-Kumar, M.S. Suresh, J. Nagaraju, IEEE Trans. Electron. Devices 48 (2001) 2177.
[2] G. Friesen, E.D. Dunlop, R. Wendt, Thin Solid Films 387 (2001).
[3] D. Chenvidhya, K. Kirtikara, C. Jivacete, Sol. Energy Mater. Sol. Cells 80 (2003) 459.
[4] L. Raniero, S. Zhang, H. Águas, I. Ferreira, R. Igreja, E. Fortunato, R. Martins, Thin Solid Films 487 (2005) 170.
[5] F. Fabregat-Santiago, J. Bisquert, G. Garcia-Belmonte, G. Boschloo, A. Hagfeldt, Sol. Energy Mater. Sol. Cells 87 (2005) 117.
[6] J. Bisquert, G. Garcia-Belmonte, Electron. Lett. 33 (1997) 900.
[7] G. Garcia-Belmonte, J. Bisquert, V. Caselles, Solid-State Electron. 42 (1998) 939.
[8] S.M. Sze, Physics of Semiconductor Devices, John Wiley and Sons, New York, 1981.
[9] H. Sakata, T. Nakai, T. Baba, M. Taguchi, S. Tsuge, K. Uchihashi, S.S. Kiyama, Proceedings of the 28th IEEE Photovoltaic Specialist Conference, Anchorage, U.S.A., 2000 (September 17–22), p. 7.
[10] N. Jensen, R.M. Hausner, R.B. Bergmann, J.H. Werner, U. Rau, Prog. Photovolt., Res. Appl. 10 (2002) 1.
[11] M. Tucci, G. de Cesare, J. Non-Cryst. Solids 338–340 (2004) 663.
[12] T.H. Wang, E. Iwaniczko, M.R. Page, Q. Wang, D.H. Levi, Y. Yan, Y. Xu, H.M. Branz, Mater. Res. Soc. Symp. Proc. 862 (2005) 413.
[13] C. Voz, D. Muñoz, M. Fonrodona, I. Martin, J. Puigdollers, R. Alcubilla, J. Escarre, J. Bertomeu, J. Andreu, Thin Solid Films, to be published.
[14] A.H. Mahan, J. Carapella, B.P. Nelson, R.S. Crandall, I. Balberg, J. Appl. Phys. 69 (1991) 6728.
[15] C. Voz, D. Muñoz, I. Martín, A. Orpella, M. Vetter, J. Puigdollers, R. Alcubilla, M. Fonrodona, D. Soler, J. Bertomeu, J. Andreu, in: W. Hoffmann, J.L. Bal, H. Ossenbrink, W. Palz, P. Helm (Eds.), Proceedings of the 19th European Photovoltaic Solar Energy Conference and Exhibition, Paris, France, 2004 (June 7–11), p. 1237.
[16] A. Werner, M. Kunst, J. Appl. Phys. 64 (1988) 211.